Analytica Chimica Acta 1231 (2022) 340439

Contents lists available at ScienceDirect

Analytica Chimica Acta

journal homepage: www.elsevier.com/locate/aca

# CRISPR/Cas12a system responsive DNA hydrogel for label-free detection of non-glucose targets with a portable personal glucose meter

Wenxiao Ma [a], Minghui Liu [a], Shupu Xie [a], Bo Liu [a], Lizhi Jiang [a], Xiaoru Zhang [a,*], Xunyi Yuan [b,**]

[a] Key Laboratory of Optic-electric Sensing and Analytical Chemistry for Life Science, MOE, Key Laboratory of Analytical Chemistry for Life Science in Universities of Shandong, Qingdao University of Science and Technology, Qingdao, 266042, PR China
[b] Department of General Surgery, Qilu Hospital (Qingdao), Cheeloo College of Medicine, Shandong University, 758 Hefei Road, Qingdao, Shandong, 266035, PR China

## HIGHLIGHTS

- Portable personal glucose meter was used to detect non-glucose targets.
- DNA hydrogel was prepared for label-free encapsulating invertase.
- CRISPR/Cas system can efficiently destroy DNA hydrogel and release invertase.
- The same crRNA can be used to detect different targets.

## GRAPHICAL ABSTRACT

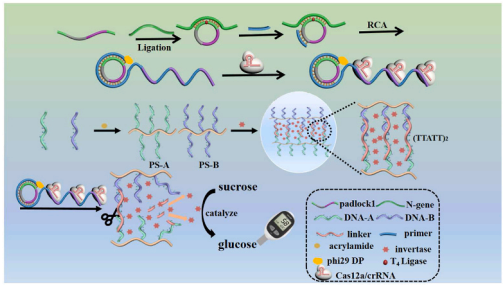


## ARTICLE INFO

*Keywords:*
Personal glucose meter
CRISPR/Cas12a
DNA hydrogel
SARS-CoV-2 N-Gene
Polychlorinated biphenyls (PCB 77)

## ABSTRACT

In this work, personal glucose meter (PGM) as a portable electrochemical device was utilized for sensitive detection of non-glucose targets: N-gene and PCB77, respectively. DNA hydrogel, which can respond to CRISPR/Cas system, was prepared for label-free encapsulating invertase. In the presence of targets, the repeated sequence for the activation of Cas12a was obtained due to the performance of RCA. Unlike "one-to-one" recognition, activated Cas12a can efficiently cleave multiple single-stranded linker DNAs on DNA hydrogels, thus releasing many invertase that can be used for PGM detection. With the amplification of RCA and CRISPR/Cas system, high detection sensitivity can be obtained even using portable PGM. The detection limits for N-gene and PCB77 were 2.6 fM and $3.2 \times 10^{-5}$ μg/L, respectively, with high specificity and good practical application performance. The developed biosensor can be used for online monitoring with the merit of low cost, easy operation and can be used for various targets analysis.

## 1. Introduction

Conventional biosensors, including fluorescence, electrochemistry, surface-enhanced Raman scattering (SERS) and surface plasmon resonance (SPR) et al., can provide accurate detection results. However, these methods require professional operators, complex and expensive

* Corresponding author.
** Corresponding author.
*E-mail addresses:* zhangxr7407@126.com (X. Zhang), yzhtyxy@163.com (X. Yuan).

https://doi.org/10.1016/j.aca.2022.340439
Received 11 August 2022; Received in revised form 20 September 2022; Accepted 22 September 2022
Available online 26 September 2022

instruments, which cannot meet the requirements for convenient, online detection and hinders their practical application to a great extent. In order to overcome the above shortcomings, people urgently need to find other analysis methods for food safety testing, health assessment, and environmental monitoring [1,2]. Colorimetry, which can observe color changes directly with the eyes, has attracted much attention in recent years [3]. But this method cannot provide digital detection information for quantitative detection. Recently, some digital detection methods, including temperature, pressure, distance, electrochemical signal, and so on, have been used in biosensors [4–9]. Among them, the personal glucose meter (PGM), as a mature electrochemical detection device, has attracted extensive research interest because of its advantages of portability, low cost, easy operation, and high accuracy. PGM can not only be used to monitor the blood glucose of diabetics but also to detect a variety of non-glucose targets, including DNA [10], cocaine [11], ATP [11,12], aflatoxin B1 [13], miRNA [14], metal ions [15] and protein biomarkers [16] et al.

To increase the sensitivity of PGM, several methods have been developed. For example, Yang et al. encapsulated a large amount of sucrase in liposomes for signal amplification [17]. Wang et al. developed a sensitive PGM sensor through the amplification of a DNA walking machine [13]. Xu et al. used an isothermal circular strand-displacement polymerization strategy to improve the sensitivity of PGM detection [18]. Loop-based DNA competitive hybridization reaction was applied by Liu's group for amplified PGM signals [19].

The CRISPR/Cas system as an adaptive immune system of archaea and bacteria has attracted much attention in the field of genome editing as well as nucleic acid-related detection [20]. Among various Cas proteins, Cas12a (Cpf1) has attracted much attention due to DNA endonuclease-targeted CRISPR trans reporter (DETECTR). The binding of the Cas12a/crRNA complex to single-stranded DNA (ssDNA) or double-stranded DNA (dsDNA) with a protospacer-adjacent motif (PAM, T–rich) sequence results in indiscriminate *trans*-cutting to surrounding ssDNA [21]. At present, CRISPR/Cas12a system has been used in the field of colorimetry [22], fluorescence [23], electrochemistry [24], electrochemiluminescence [25], photoelectrochemistry [26] and Raman [27] et al. Recently, CRISPR-Cas12a amplified PGM sensor was developed for the detection of microRNA [28] and SARS-CoV-2 [29]. These works required the modification of invertase with DNA. Such modification will complicate the sensing procedure and may influence enzyme activity to a certain extent. Consequently, a label-free strategy for CRISPR/Cas12a triggered PGM sensor is urgently needed.

DNA hydrogel has the characteristics of good biocompatibility, portability, and mechanical stability. Recently, Li's group prepared hydrogel based on DNA tetrahedron for sensing DNA methyltransferase using PGM [30]. Yang's group synthesized "sweet" hydrogel to detect small molecules with PGM [11]. Based on these works, we designed a smart DNA hydrogel to overcome the one-to-one recognition of a target molecule to a DNA strand in the DNA hydrogel and improve detection sensitivity as well as expand the range of object. This DNA hydrogel can respond to CRISPR/Cas12a system and release the encapsulated invertase for PGM detection. Here, SARS-CoV-2 N-gene (nucleocapsid phosphoprotein gene) and PCB77 (3,3′,4,4′- tetrachlorobiphenyl) were selected as model targets. The former is an essential marker for COVID-19 viral infection [31], and the latter is a highly toxic environmental persistent organic pollutant [32]. These two targets are selected to prove that the proposed sensor can be used to detect different types of targets. By ingenious design of DNA sequences, the same crRNA can be used to detect two completely different targets.

## 2. Experimental section

### 2.1. Preparation of the invertase-encapsulated DNA hydrogel

DNA Hydrogel was prepared according to previous literature with some modifications [33,34]. Solution A and B were prepared at first. Solution A consisted of 10 mM Tris, 200 mM NaCl, 1 mM EDTA and 4% acrylamide (pH 8.0). Next, 0.01 g $(NH_4)_2S_2O_8$, 5 μL N,N,N′, N′-Tetramethylethylenediamine (TEMED) were added to 100 μL DEPC water to form solution B. The acrydite-modified DNA-A and DNA-B were diluted to 100 μM with solution A, respectively, and then placed in a vacuum desiccator at 37 °C for 10 min to remove air. Then, the newly prepared solution B was added to the solution of DNA-A or DNA-B at a ratio of 0.014:1 (V: V). Finally, the mixture was put in a vacuum desiccator again at 37 °C for 15 min to give the polymer strands A (PS-A) and the polymer strands B (PS–B), respectively.

To the mixture of PS-A, PS-B, and invertase, the linker DNA was added. The ratio of the PS-A, PS-B, and the linker DNA was 1:1:1. The final concentration of invertase was 0.025 μg/μL. After vigorous shaking, the obtained homogeneous solution was reacted at 50 °C for 5 min, followed by cooled naturally to 25 °C to give invertase-encapsulated DNA hydrogel.

### 2.2. Rolling circle amplification (RCA) assay

First, 10 μM padlock 1, 10 μM primer and different concentrations of N-genes in 1 × T4 DNA ligase buffer were annealed at 95 °C for 5 min and slowly cooled down to 25 °C. Then T4 ligase was added to make a final concentration of 10 U/μL. After incubation at 16 °C for 2 h, the mixture was heated to 65 °C for 10 min to denature ligase and then cooled down slowly. To 10 μL of the reaction solution obtained above, phi29 DNA polymerase (phi 29 DP, final concentration 1 U/μL), 2 mM dNTP, 1 × phi29 DP buffer, and 1 × BSA were added and reacted at 30 °C for 2 h.

### 2.3. CRISPR/Cas12a assay

15 μL mixture containing Cas12a (200 nM), crRNA (300 nM), RNase inhibitor (5 U) and 1 × NEBuffer 2.1 (50 mM NaCl, 10 mM Tris-HCl, 10 mM $MgCl_2$, 100 μg/ml BSA, pH 7.9) was incubated at 37 °C for 30 min. After adding 5 μL of RCA product, the mixture was homogenized by oscillation and then added to 10 μL DNA hydrogel. Finally, the mixture was reacted at 37 °C for 1 h.

### 2.4. PGM assay

The mixture containing 10 μL supernatant from Cas12a treated DNA hydrogel obtained above, 30 μL of 1 M sucrose, 6 μL of 0.1 M sodium citrate buffer (pH 5.6) and 4 μL deionized water was incubated at 37 °C for 30 min. Then, 5 μL solution was pipetted for PGM analysis.

### 2.5. PCB77 detection

Firstly, PCB77 was dissolved in DMSO (5%) and then diluted with DEPC water. In the detection process, 1 μM PCB77 aptamer and 1 μM cDNA were annealed at 95 °C for 5 min, and naturally cooled down to 25 °C to form double-stranded DNA. Then, different concentrations of PCB77 were added and reacted at 37 °C for 2 h. The replaced cDNA can be used to initiate RCA reaction in the presence of padlock2. Finally, Cas12a activation and PGM detection were performed as described above.

## 3. Results and discussion

### 3.1. Working principle of the developed biosensor

As for the detection of N-gene, the biosensor platform involves two essential processes. One is the pre-amplification *via* RCA process and the activation of Cas12a. The other is the dissociation of DNA hydrogels and PGM detection. As shown in Scheme 1, padlock 1 consisted of an N-gene recognition part (green color), a universal non-trigger DNA strand (NTS, purple color) and a complementary sequence of primer (gray color).

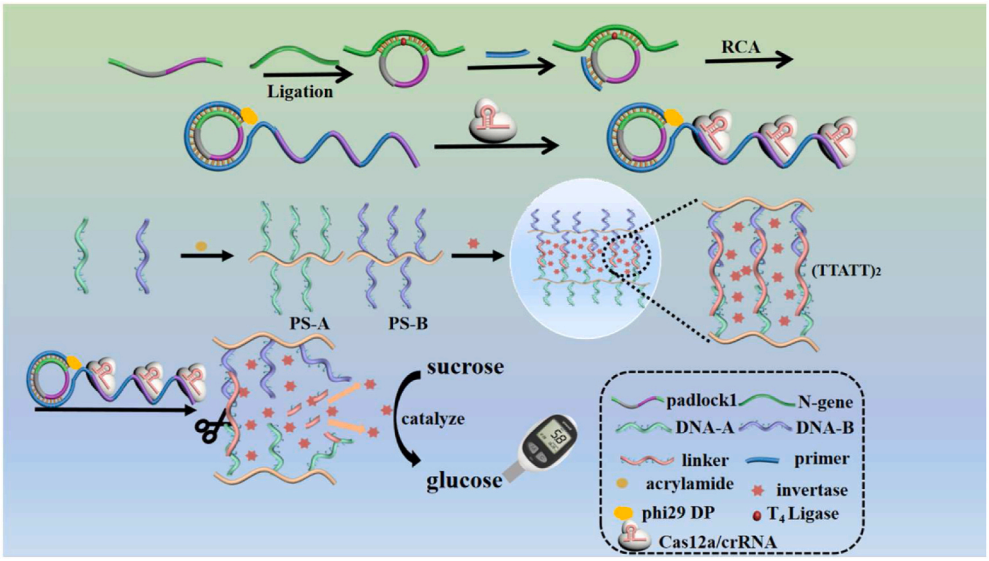


**Scheme 1.** Schematic representation of the DNA hydrogel sensing platform for sensing N-gene *via* a PGM.

Specifically, when target N-gene was present, it hybridized with padlock 1 and induced the circularization with the assistance of T4 DNA ligase. Next, the RCA reaction occurs in the presence of primer and phi 29 DP to generate long DNA amplicons with repeated trigger DNA strands (TS, purple color). The TS fraction could activate Cas12a after hybridization with crRNA, which triggered the *trans*-cleavage process for single-stranded DNA. When detecting different target genes, only the recognition part of the padlock DNA strand needs to be replaced and the NTS sequence remains unchanged. In this way, we can detect different target sequences with the same crRNA.

In the detection step, polymer strands A (PS-A) was prepared through copolymerization of acrydited DNA-A with acrylamide. When acrydite-

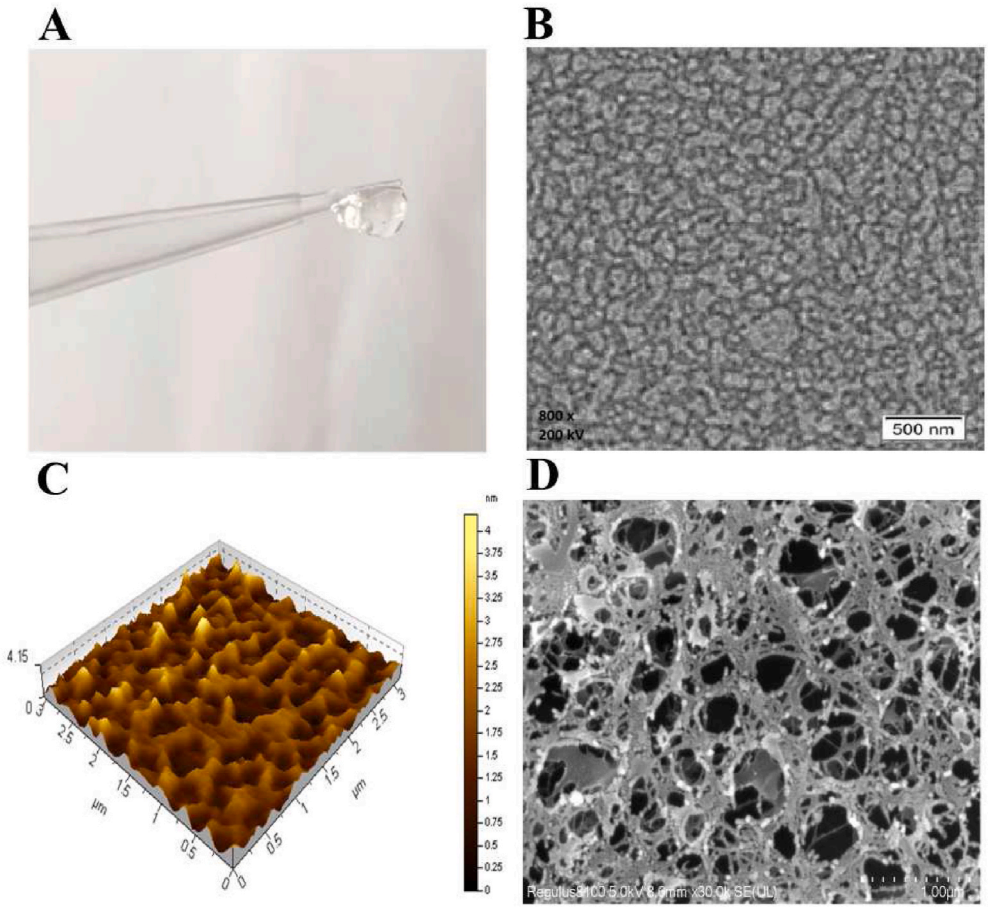


**Fig. 1.** Characterization of DNA hydrogels (A) Image of a piece of transparent gelatinous DNA hydrogel; TEM (B) and AFM (C) images of DNA hydrogel; (D) SEM image of lyophilized DNA hydrogel.

modified DNA-B was used instead, PS-B could be obtained by the same method. Then the invertase-embedded 3D DNA hydrogel was obtained after the hybridization of linker DNA with DNA on the side chain of PS-A and PS-B in the presence of invertase. It should be noted that in addition to the binding parts with PS-A and PS-B side chains, linker DNA also has some single-stranded sequences remaining (TTATTTTATT), which can be cut by the activated Cas12a obtained above. The nonspecific *trans*-cleavage activity triggers the cleavage of ssDNA in the DNA hydrogel network. The breakdown of the DNA hydrogel network will release the encapsulated invertase, which can catalyze the hydrolysis of sucrose to glucose. Thus, quantitative detection of target RNA can be achieved by measuring the produced glucose in the supernatant with a PGM.

### 3.2. Formation of DNA hydrogel

The formation of polymer strands PS-A and PS-B can be verified by agarose gel electrophoresis. As shown in Fig. S1, both PS-A and PS-B were at the top of the electrophoresis lane, suggesting the successful formation of the polymer. On the other hand, the hybridization of DNA-A, DNA-B and linker DNA was confirmed by polyacrylamide gel electrophoresis (Fig. S2). After incubation of PS-A and PS-B with linker DNA, the sample lost fluidity and formed a gelatinous form at the bottom of the EP tube (Fig. S3). When lifted with a pipette tip, a transparent gelatinous mass could be found (Fig. 1A). The zeta potential of the DNA hydrogel shown in Fig. S4 was more negative compared to that of PS-A and PS-B. The morphology of prepared DNA hydrogel was characterized by transmission electron microscopy (TEM), atomic force microscopy (AFM), and scanning electron microscopy (SEM). As shown in Fig. 1B and C, a 3D network-like structure was observed. The height of the gel fibers was about 2 nm (Fig. S5). The SEM image of the lyophilized DNA hydrogels in Fig. 1D showed a perfectly porous structure. All these proved that DNA hydrogel was prepared successfully.

### 3.3. The detection feasibility

The detection process includes RCA amplification, the activation of Cas12a system, the release of invertase due to the breakdown of the DNA hydrogel, and PGM detection. Gel electrophoresis showed that padlock1 could hybridize with N-gene and primer, followed by initiating RCA reaction under the catalysis T4 DNA ligase and phi29 DP (Fig. S6 and Fig. S7). Subsequently, the activation of Cas12a/crRNA system could be verified by the *trans*-cleavage of fluorophore and quencher labeled ssDNA (FQ) reporters. As shown in Fig. 2A, without target N-gene, no fluorescence for FQ reporters was found (black curve). In the presence of the N-gene, the RCA reaction could be triggered to produce long-stranded DNA with a repetitive sequence, which can be used to activate Cas12a. The fluorescence intensity increased significantly due to the *trans*-cleavage activity of Cas12a (red curve).

The dissociation of DNA hydrogel could be demonstrated using Au NPs (Fig. S8**)** encapsulated in the hydrogel. As shown in Fig. 2B, when adding water to Au NPs encapsulated in DNA hydrogel, obvious stratification could be seen. After adding activated LbCas12a into DNA hydrogel, *trans*-cleavage of the ssDNA led to the fracture of DNA hydrogel. Hence, a homogeneous Au NPs solution was formed. The dissociation of DNA hydrogel could also be verified through the SEM image of DNA hydrogel after being cut by CRISPR/Cas12a (Fig. S9**)**.

In PGM detection, we conducted the following control experiments. As shown in Fig. 2C, when detecting DNA hydrogel unencapsulated invertase in the presence of sucrose (column a) or DNA hydrogel encapsulated invertase but without sucrose (column b), no glucose signals were observed because both the enzyme and the substrate are indispensable. When in the presence of sucrose and DNA hydrogel encapsulated invertase, but in the absence of Cas12a (column c) or target N-gene (column d), only a weak glucose signal could be found due to the reaction of sucrose with a small amount of invertase on the surface of DNA hydrogel. High glucose signals could be observed only when sucrose, invertase, Cas12a and target N-gene ($1.0 \times 10^{-9}$ M) all existed. This demonstrates the feasibility of the developed PGM biosensor.

### 3.4. Optimization of experimental condition

Conditions optimization of for the RCA reaction was investigated in Supporting information. From the results shown in Fig. S10, the optimal time for the RCA reaction was 120 min, and the optimal concentration of the phi29 DP was 1 U/μL. In the CRISPR/Cas12a system, the ratio of Cas12a to crRNA can affect the enzyme's catalytic activity. As shown in Fig. 3A, when the ratio of Cas12a to crRNA was selected as 1: 1.5, PGM signal was the highest. So, Cas12a: crRNA = 1: 1.5 was used in the following experiments. Subsequently, the reaction time of sucrose catalyzed by invertase was optimized. As shown in Fig. 3B, the PGM signal basically did not increase after 30 min, indicating 30 min was the best incubation time. The amount of invertase plays a crucial role in the catalytic effect. A low concentration of invertase leads to low catalytic efficiency and small PGM signals. While high concentrations of invertase can produce extensive backgrounds as well as over-range signals. Here, four concentrations of invertase were investigated. From the results shown in Fig. 3C and Fig. S11, the optimal concentration of encapsulated invertase was 0.025 μg/μL.

Furthermore, DNA hydrogel can be cleaved by activated Cas12a. The reaction kinetics is related to the concentration of the target N-gene. The higher the concentration of N-gene, the more activation strands will be generated, thus the activated Cas12a will destroy more DNA hydrogels. As shown in Fig. 3D, the PGM signal could reach its maximum within 1 h, even in the presence of the 10 fM N-gene.

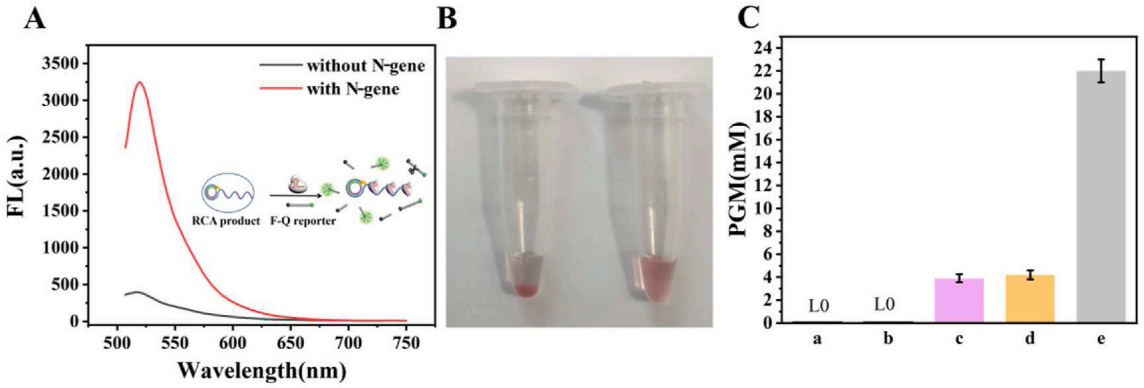


**Fig. 2.** The feasibility of the proposed method. (A) The cleavage of FQ reporters by Cas12a/crRNA system. Concentrations of target N-gene and FQ reporter were $1.0 \times 10^{-9}$ M and 1.6 μM, respectively. (B) The image of Au NPs encapsulated in DNA hydrogel with water (left) and activated Cas12a (right). (C) PGM detection under different conditions.

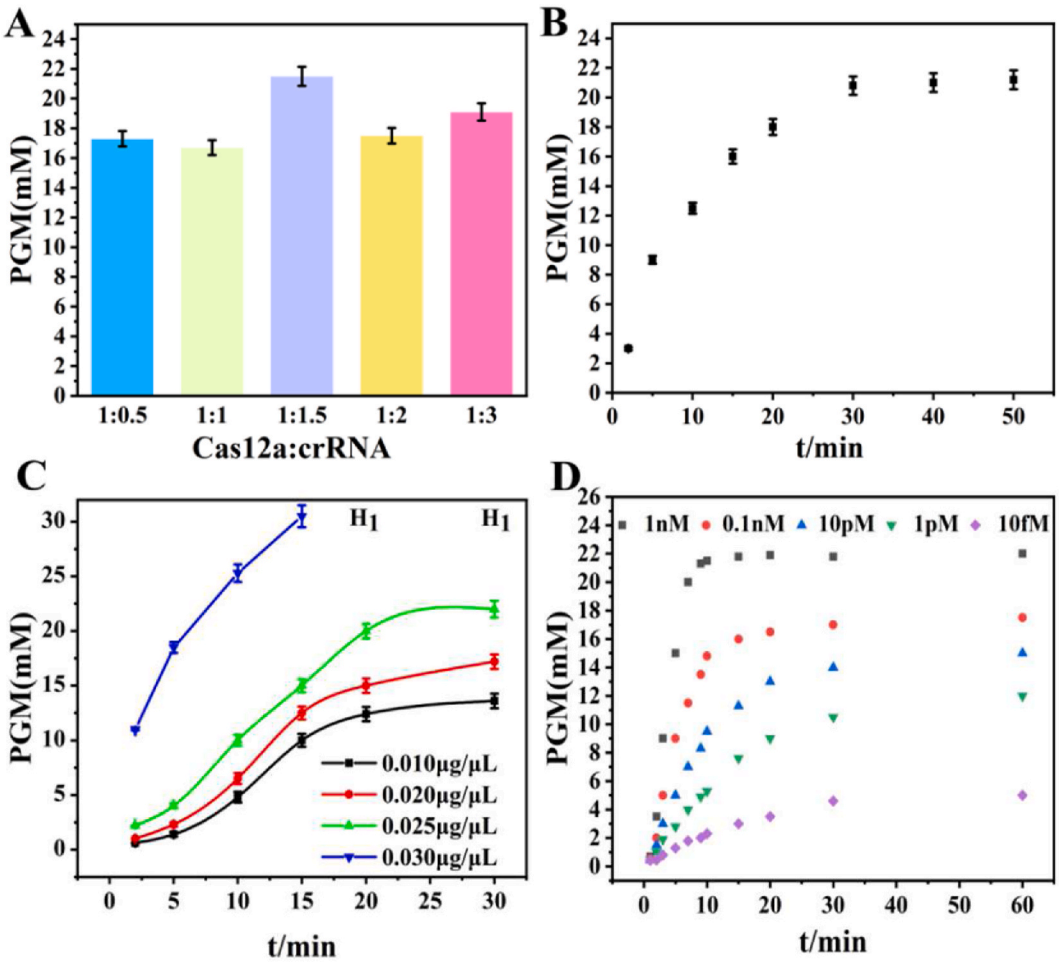


**Fig. 3.** Optimization of experimental conditions. (A) PGM signals using different ratios of Cas12a to crRNA. (B) The reaction time of sucrose with the degraded DNA hydrogel. (C) Changes in PGM signal over time due to different amounts of invertase encapsulated in DNA hydrogels. The concentration of N-gene is $1.0 \times 10^{-9}$ M. (D) Kinetics of DNA hydrogels cleaved by Cas12a in the presence of different concentrations of N- gene.

### *3.5. Detection of N-gene*

Under optimal experimental conditions, different concentrations of N-gene were applied. After RCA and Cas12a shearing, the supernatant reacted with sucrose, followed by PGM detection. As shown in Fig. 4A, significantly increased PGM signals could be observed with the increase of N-gene concentration. The PGM signal showed a linear relationship with the logarithm of N-gene concentration ranging from 10 fM-1.0 nM. The reproducibility was investigated by five repetitive measurements of 1.0 pM N-gene with a relative standard deviation (RSD) of 3.7%, and the limit of detection (LOD) was 2.6 fM with an $R^2$ of 0.995. Compared to previously reported methods for N-gene determination (shown in Table S3 of Supporting Information), we found that relatively sensitive detection results could be obtained by using portable PGM after amplification with RCA and CRISPR technology.

The selectivity of the developed CRISPR-PGM biosensor was investigated in Fig. 4B. Compared to the blank sample, there was almost no difference in the PGM signal for random sequence ($1.0 \times 10^{-9}$ M). While the PGM signal of $1.0 \times 10^{-9}$ M N-gene increased significantly. The PGM signals for the same concentration of one-base (M1), two-base (M2), and three-base mismatched DNA (M3) decreased obviously. These proved that the developed CRISPR-PGM sensor has good selectivity, even for single-base mutated genes.

It is well known that PGM is a device used to monitor blood glucose by diabetic patients. Therefore, whether the developed method can be used to determine the N-gene in diabetic blood is an unavoidable problem. To overcome this problem, glucose oxidase (GOx) was added to remove the pre-existing endogenous glucose, and then denature the GOx before the test (see Fig. S12). Here, glucose was added to the buffer to mimic the pre-existing endogenous glucose. The final concentration of glucose was 10 mM. Then $1.0 \times 10^{-12}$ M N-gene was added as a detection sample. Subsequently, 0.1 mg/mL GOx was added to the sample solution and reacted at 25 °C for 20 min. Then, the mixture was heated at 95 °C for 10 min to deactivate GOx. The detection procedure was carried out as described previously. The results shown in Fig. 4C suggested that without pretreatment, the PGM signal for N-gene in glucose solution was relatively high (green column). While in the presence of the same amount of N-gene, the measured value after pretreatment with GOx (orange column) was in good agreement with that after subtracting the background of glucose solution (purple column). This means the developed PGM method can be used for genetic analysis of diabetic patients.

Because it is difficult for our laboratory to obtain actual samples from patients infected with Covid-19, saliva and human serum, which are usually used as SARS-CoV-2 matrixes, were selected to test the clinical diagnosis of the developed method. It should be noted that the amount of glucose in the saliva is much lower than in serum. This was confirmed by the detection results of PGM (Fig. S13). Here, three concentrations of N-gene were added to buffer, saliva, human serum and 0.1 mg/mL Gox pretreated human serum. Fig. 4D showed that the PGM signals detected in human serum were higher than others due to the presence of glucose in serum. While the PGM signals were identical for N-gene spiked in the

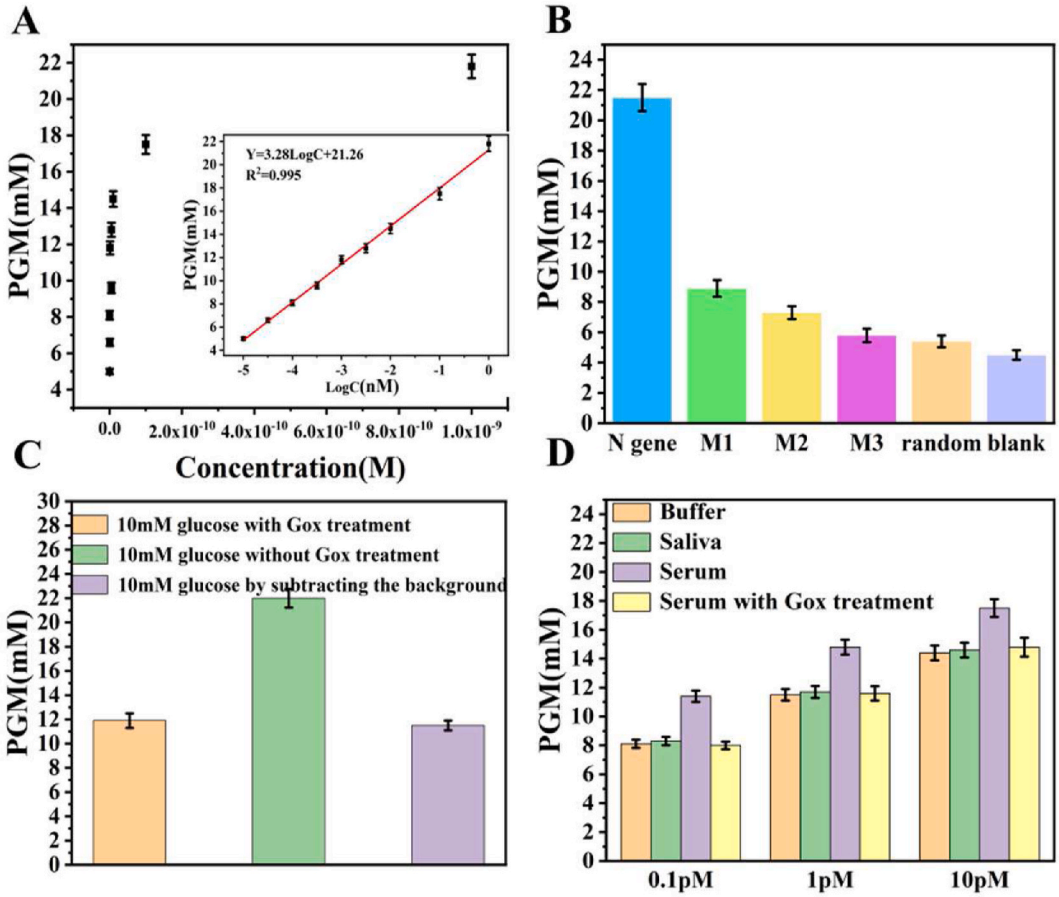


**Fig. 4.** Analysis of N-gene using CRISPR-PGM system. (A) The relationship of the PGM signals with different concentrations of N-gene. Insert: linear calibration curve between the PGM signals and logarithm of N-gene concentrations. (B) Selectivity of the assay for N-gene. The concentrations of different sequences were $1.0 \times 10^{-9}$ M. (C) Detection $1.0 \times 10^{-12}$ M N-gene in the solution containing 10 mM glucose under different conditions. (D) Detection of three concentrations of N-gene in buffer, saliva, human serum, and GOx pretreated human serum. An error bar represents the error for three independent experiments.

buffer, saliva, and GOx pretreated human serum matrixes, suggesting this method can be used to detect the actual samples of complex systems. On the other hand, after storing 2 weeks in the refrigerator, the performance of the invertase-encapsulated DNA hydrogels basically did not change, which proved the excellent storage stability of the prepared DNA hydrogels (Fig. S14).

### 3.6. Detection of PCB77

To verify the generality of the CRISPR-PGM sensor biosensor, we extended our detection from a gene to a small molecule. PCB77, as one of the most poisonous dioxin-like polychlorinated biphenyl, not only hazards ecosystems but threatens public health. In order to realize the assay of PCB77, first, the aptamer of PCB77 was hybridized with its complementary strand cDNA to form a stable dsDNA structure. In the presence of PCB77, the recognition between PCB77 and its aptamer led

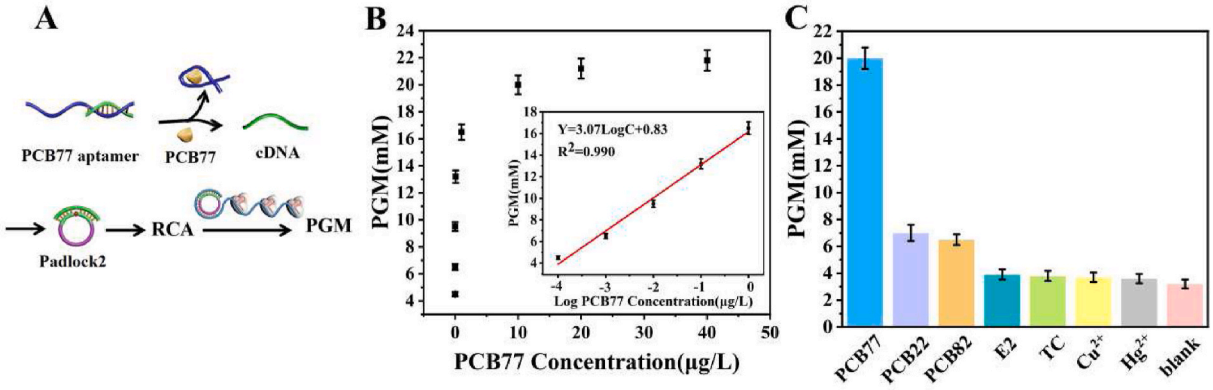


**Fig. 5.** (A) Schematic illustration for PCB77 detection. (B) The relationship between the PGM signal and logarithm of PCB77 concentrations. (C) Selectivity for PCB77 detection.

to the dehybridization of dsDNA and the releasement of cDNA, which was used as a primer to initiate RCA reaction (Fig. 5A). Subsequently, CRISPR-PGM sensor biosensor based on DNA hydrogel was performed as that of N-gene. It should be noted, during the detection of PCB 77, padlock2 was used, which consisted of a cDNA recognition part and a same universal NTS part as that for N-gene detection. After RCA, long DNA amplicons with the same repeated TS sequences were produced. Therefore, the same crRNA could be used for the activation of Cas12a.

The complementary base number between aptamer and cDNA is a significant element in sequence design. The low number of complementary bases leads to low hybridization efficiency and high detection background. However, the high number of complementary bases makes it difficult for the recognition of aptamer with PCB77, giving low detection signal. Here, aptamer and cDNA of different complementary bases were compared. After recognition with 10 μg/L PCB77, RCA and activation of Cas12a, the change of fluoresce signal due to *trans*-cleavage of FQ reporter before and after addition PCB77 was measured. From the results shown in Fig. S15, cDNA containing 20 complementary bases was used in the following experiments. The binding of PCB77 to its aptamer can be verified by the fluorescence quenching-recovery test (Fig. S16).

The performance of developed aptasensor for the detection of PCB77 was studied (Fig. 5B). The PGM signal showed a linear relationship with the logarithm of PCB 77 concentration ranging from $1.0 \times 10^{-4}$ to 1.0 μg/L ($R^2 = 0.990$). The detection limit for PCB 77 was calculated to be $3.2 \times 10^{-5}$ μg/L, which is below the maximum dose of PCB77 (0.5 ppb) in drinking water fixed by the Environmental Protection Agency. Compared to previous works, the sensitivity of the proposed Cas12a-PGM method is acceptable (Table S4).

In order to investigate the selectivity of the aptasensor, other interfering substances, including PCB22, PCB82, 17β-estradiol (E2), tetracycline (TC), $Cu^{2+}$, and $Hg^{2+}$, were compared. The concentration of all substances was 10 μg/L. The significantly high signal in Fig. 5C demonstrated that the prepared aptasensor has high specificity toward PCB77.

To confirm the practical performance of the sensor, different amounts of PC77 were added to tap water and water from Li Cun River (Qingdao, China) by the standard addition method. For river water, pretreatment is required before testing. Firstly, the river water samples were centrifuged, filtered with a 0.22 μm filter membrane, and diluted 100 times with 0.1 M PBS. Subsequently, three concentrations of PCB77 (10, 50, and 100 ng/L), were spiked into the water samples, respectively. As compared in Table S5, the results of this method coincided with those by GC-MS. The recovery of these two methods was between 95 and 105%, and the RSD of parallel tests was less than 5% (n = 3). This indicates that the prepared aptasensor can be successfully used for PCB77 analysis in complex actual environmental water samples. The calculation of F-test and T-test (see Supporting information) showed that there was no significant difference between the results of this work and those of the standard method GC-MS, and their correctness was in accordance with the standard requirements.

## 4. Conclusion

In this work, a label-free strategy for CRISPR/Cas12a triggered portable PGM sensor was developed for the detection of two kinds of targets. A smart DNA hydrogel encapsulating invertase was prepared. After target recognition and RCA reaction, repeated sequences for Cas12a activation were generated. Then activated Cas12a led to efficient cleavage of DNA hydrogel. Under these two amplifications, many invertase was released for PGM detection in the presence of very few targets. Here, targets N-gene and PCB77 can be detected sensitively with high selectivity. By clever design, the same crRNA can be used to detect different targets, reducing detection costs and improving detection universality. Furthermore, the developed sensor can be used for real sample detection. This work provides a simple and sensitive method, which can be easily used in the online detection of various analysts. However, the use of the RCA method, although simple to operate, increases the detection time and is not conducive to the requirements of the rapid assay. Adjustments can be made later to meet the requirements of point-of-care testing (POCT).

## CRediT authorship contribution statement

**Wenxiao Ma:** Performed experiments, analyzed the results, wrote the original draft. **Minghui Liu:** Investigation, Data curation. **Shupu Xie:** Methodology, Data curation, Software. **Bo Liu:** Conceptualization, Validation. **Lizhi Jiang:** Methodology, Formal analysis. **Xiaoru Zhang:** Project administration, Funding acquisition, Writing – review & editing. **Xunyi Yuan:** Conceptualization, Writing – review & editing.

## Declaration of competing interest

The authors declare that they have no known competing financial interests or personal relationships that could have appeared to influence the work reported in this paper.

## Data availability

No data was used for the research described in the article.

## Acknowledgments

This work was supported by the National Natural Science Foundation of China (22276103, 21775080), Qingdao Outstanding Health Professional Development Fund, Scientific Reuter Foundation of Qilu Hospital of Shandong University (Qingdao) (No. QDKY2016QN04) and Elites Program of Qilu Hospital of Shandong University.

## Appendix A. Supplementary data

Supplementary data to this article can be found online at https://doi.org/10.1016/j.aca.2022.340439.

## References

[1] C. Moore, Point-of-care tests for infection control: should rapid testing be in the laboratory or at the front line? J. Hosp. Infect. 85 (2013) 1–7.
[2] W. Sow, T. Ye, F.C. Zhang, H. Li, Smart materials for point-of-care testing: from sample extraction to analyte sensing and readout signal generator, Biosens. Bioelectron. 170 (2020), 112682.
[3] X. Zhang, Y. Zhang, F. Chen, Visual detection of single-nucleotide polymorphisms and DNA methyltransferase based on cation-exchange of CuS nanoparticles and click chemistry of functionalized gold nanoparticles, Chem. Commun. 52 (2016) 13261–13264.
[4] Z. Yu, G. Cai, X. Liu, Platinum nanozyme-triggered pressure-based immunoassay using a three-dimensional polypyrrole foam-based flexible pressure sensor, ACS Appl. Mater. Interfaces 12 (2020) 40133–40140.
[5] J. Zhang, H. Xing, Y. Lu, Translating molecular detections into a simple temperature test using a target-responsive smart thermometer, Chem. Sci. 9 (2018) 3906–3910.
[6] J. Oh, K. Chow, Naked-eye coulometric sensor using a longitudinally oriented Ag band electrode in a microfluidic channel, Anal. Chem. 88 (2016) 4849–4856.
[7] X. Liu, H. Cheng, Y. Zhao, Y. Wang, F. Li, Portable electrochemical biosensor based on laser-induced graphene and $MnO_2$ switch-bridged DNA signal amplification for sensitive detection of pesticide, Biosens. Bioelectron. 199 (2022) 113906–113913.
[8] X. Liu, X. Li, X. Gao, L. Ge, X. Sun, F. Li, A universal paper-based electrochemical sensor for zero-background assay of diverse biomarkers, ACS Appl. Mater. Interfaces 11 (2019) 15381–15388.
[9] X. Liu, X. Gao, L. Yang, Y. Zhao, F. Li, Metal–organic framework-functionalized paper-based electrochemical biosensor for ultrasensitive exosome assay, Anal. Chem. 93 (2021) 11792–11799.
[10] Y. Jia, F. Sun, N. Na, J. Ouyang, Detection of p53 DNA using commercially available personal glucose meters based on rolling circle amplification coupled with nicking enzyme signal amplification, Anal. Chim. Acta 1060 (2019) 64–70.
[11] L. Yan, Z. Zhu, Y. Zou, Target-responsive "sweet" hydrogel with glucometer readout for portable and quantitative detection of non-glucose targets, J. Am. Chem. Soc. 135 (2013) 3748–3751.
[12] J. Ahn, H. Kim, K. Park, A personal glucose meter for label-free and washing-free biomolecular detection, Anal. Chem. 90 (2018) 11340–11343.

[13] X. Yang, D. Shi, S. Zhu, Portable aptasensor of aflatoxin B1 in bread based on a personal glucose meter and DNA walking machine, ACS Sens. 3 (2018) 1368–1375.
[14] X. Huang, J. Li, M. Lu, W. Zhang, Z. Xu, B. Yu, J. Tian, Point-of-care testing of MicroRNA based on personal glucose meter and dual signal amplification to evaluate drug-induced kidney injury, Anal. Chim. Acta 1112 (2020) 72–79.
[15] W. Xiao, Y. Gao, Y. Zhang, Enhanced 3D paper-based devices with a personal glucose meter for highly sensitive and portable biosensing of silver ion, Biosens. Bioelectron. 137 (2019) 154–160.
[16] H. Shi, J. Zheng, Y. Wang, Point-of-care testing of protein biomarkers by integrating a personal glucose meter with a concatenated DNA amplifier, Sens. Actuators B Chem. 322 (2020), 128659.
[17] B. Lin, D. Liu, J. Yan, Enzyme-encapsulated liposome-linked immunosorbent assay enabling sensitive personal glucose meter readout for portable detection of disease biomarkers, ACS Appl. Mater. Interfaces 8 (2016) 6890–6897.
[18] X. Xu, K. Liang, J. Zeng, Portable and sensitive quantitative detection of DNA based on personal glucose meters and isothermal circular strand-displacement polymerization reaction, Biosens. Bioelectron. 64 (2015) 671–675.
[19] Y. Shan, Y. Zhang, W. Kang, Quantitative and selective DNA detection with portable personal glucose meter using loop-based DNA competitive hybridization strategy, Sens. Actuators B Chem. 282 (2019) 197–203.
[20] J. Chen, E. Ma, L. Harrington, C. Da, X. Tian, J. Palefsky, J. Doudna, CRISPR-Cas12a target binding unleashes indiscriminate single-stranded DNase activity, Science 360 (2018) 436–439.
[21] S. Wang, Y. Du, D. Wang, Signal amplification and output of CRISPR/Cas-based biosensing systems: a review, Anal. Chim. Acta 1185 (2021), 338882.
[22] Y. Li, H. Mansour, T. Wang, S. Poojari, F. Li, Naked-Eye detection of grapevine red-blotch viral infection using a plasmonic CRISPR Cas12a assay, Anal. Chem. 91 (2019) 11510–11513.
[23] P. Wang, Y. Liu, Y. Yu, Y. Zhang, J. Peng, L. Niu, J. Zhang, Hydrazone ligation assisted DNAzyme walking nanomachine coupled with CRISPR-Cas12a for lipopolysaccharide analysis, Anal. Chim. Acta 1174 (2021), 338747.
[24] D. Zhang, Y. Yan, H. Que, T. Yang, X. Cheng, S. Ding, X. Zhang, W. Cheng, CRISPR/Cas12a-Mediated interfacial cleaving of hairpin DNA reporter for electrochemical nucleic acid sensing, ACS Sens. 5 (2020) 557–562.
[25] Z. Xu, Z. Zhao, H. Wang, S. Wang, H. Chen, J. Xu, CRISPR-Cas12a-based efficient electrochemiluminescence biosensor for ATP detection, Anal. Chim. Acta 1188 (2021), 339180.
[26] H. Shen, A. Qileng, H. Yang, H. Liang, H. Zhu, Y. Liu, H. Lei, W. Liu, Dual-signal-on" integrated-type biosensor for portable detection of miRNA: cas12a-induced photoelectrochemistry and fluorescence strategy, Anal. Chem. 93 (2021) 11816–11825.
[27] J. Choi, M. Shin, L. Yang, B. Conley, J. Yoon, S. Lee, K. Lee, J. Choi, Clustered regularly interspaced short palindromic repeats-mediated amplification free detection of viral DNAs using surface enhanced Raman spectroscopy-active nanoarray, ACS Nano 15 (2021) 13475–13485.
[28] S. Gong, J. Li, W. Pan, N. Li, B. Tang, Duplex-specific nuclease-assisted CRISPR-cas12a strategy for MicroRNA detection using a personal glucose meter, Anal. Chem. 93 (2021) 10719–10726.
[29] R. Liu, Y. Hu, Y. He, T. Lan, J. Zhang, Translating daily COVID-19 screening into a simple glucose test: a proof of concept study, Chem. Sci. 12 (2021) 9022–9030.
[30] X. Gao, X. Li, X. Sun, J. Zhang, Y. Zhao, X. Liu, F. Li, DNA tetrahedra-cross-linked hydrogel functionalized paper for onsite analysis of DNA methyltransferase activity using a personal glucose meter, Anal. Chem. 92 (2020) 4592–4599.
[31] Z. Song, Y. Ma, M. Chen, A. Ambrosi, C. Ding, X. Luo, Electrochemical biosensor with enhanced antifouling capability for COVID-19 nucleic acid detection in complex biological media, Anal. Chem. 93 (2021) 5963–5971.
[32] B. Zhang, P. Tian, H. Zhu, L. Xie, P. Dai, B. He, Ultrasensitive detection of PCB77 based on Exonuclease III-powered DNA walking machine, J. Hazard Mater. 416 (2021), 125831.
[33] Q. Wang, Y. Hu, N. Jiang, J. Wang, M. Yu, X. Zhuang, Preparation of aptamer responsive DNA functionalized hydrogels for the sensitive detection of α-fetoprotein using SERS method, Bioconjugate Chem. 31 (2020) 813–820.
[34] Y. He, X. Yang, R. Yuan, Y. Chai, Switchable target-responsive 3D DNA hydrogels as a signal amplification strategy combining with SERS technique for ultrasensitive detection of miRNA 155, Anal. Chem. 89 (2017) 8538–8544.